Lower Grade Gliomas: Relationships Between Metabolic and Structural Imaging with Grading and Molecular Factors

Marco Riva[1,3], Egesta Lopci[4], Antonella Castellano[9], Laura Olivari[4], Marcello Gallucci[10], Federico Pessina[3], Bethania Fernandes[5], Matteo Simonelli[6,11], Pierina Navarria[7], Marco Grimaldi[8], Roberta Rudà[13], Angelo Castello[4], Marco Rossi[3], Tommaso Alfiero[3], Riccardo Soffietti[13], Arturo Chiti[4,12], Lorenzo Bello[2,3]

BACKGROUND: **Positron emission tomography (PET) is a valuable tool for the characterization of brain tumors in vivo. However, few studies have investigated the correlation between carbon-11-methionine (11C-METH) PET metrics and the clinical, radiological, histological, and molecular features of patients affected by lower grade gliomas (LGGs). The present observational study evaluated the relationships between 11C-METH PET metrics and structural magnetic resonance imaging (MRI) findings with the histomolecular biomarkers in patients with LGGs who were candidates for surgery.**

METHODS: **We enrolled 96 patients with pathologically proven LGG (51 men, 45 women; age 44.1 ± 13.7 years; 45 with grade II, 51 with grade III), who had been referred from March 2012 to January 2015 for tumor resection and had undergone preoperative 11C-METH PET. The semiquantitative metrics for 11C-METH PET included maximum standardized uptake value (SUVmax), SUV ratio to normal brain, and metabolic tumor burden (MTB). The PET semiquantitative metrics were analyzed and compared with the MRI features, histological diagnosis, isocitrate dehydrogenase-1/2 status, and 1p/19q codeletion.**

RESULTS: **Histological grade was associated with SUVmax ($P = 0.002$), SUV ratio ($P = 0.011$), and MTB ($P = 0.001$), with grade III lesions showing higher values. Among the nonenhancing lesions on MRI, SUVmax ($P = 0.001$), SUV ratio ($P = 0.003$) and MTB ($P < 0.001$) were significantly different statistically for grade II versus grade III. The MRI lesion volume correlated poorly with MTB ($r^2 = 0.13$). The SUVmax and SUV ratio were greater ($P < 0.05$) in isocitrate dehydrogenase-1/2 wild-type lesions, and the SUV ratio was associated with the presence of the 1p19q codeletion.**

CONCLUSIONS: **The 11C-METH PET metrics correlated significantly with histological grade and the molecular profile. Semiquantitative PET metrics can improve the preoperative evaluation of LGGs and thus support clinical decision-making.**

INTRODUCTION

The World Health Organization (WHO) grade II and III gliomas are tumors of the central nervous system defined as lower grade gliomas (LGGs) by their clinical behavior and molecular stratification.[1-3] The updated WHO classification considered both histological and molecular parameters as crucial for an integrated diagnosis.[1] However, the coexistence of areas with different histological and biological characteristics in the same tumor can impair the correct diagnosis.

Key words
- Clinical trials observational study
- MRI
- PET
- Primary brain tumor
- Surgical therapy for tumor

Abbreviations and Acronyms
11C-METH: Carbon-11-methionine
1p19q: Chromosome arms 1p and 19q
IDH: Isocitrate dehydrogenase
LGG: Lower grade glioma
MTB: Metabolic tumor burden
PET: Positron emission tomography
ROI: Region of interest
SUV: Standardized uptake value
WHO: World Health Organization

From the Departments of [1]Medical Biotechnology and Translational Medicine, and [2]Oncology and Hemato-Oncology, Università degli Studi di Milano, Milan; [3]Unit of Oncological Neurosurgery, [4]Unit of Nuclear Medicine, [5]Unit of Pathology, [6]Humanitas Cancer Center, [7]Unit of Radiotherapy and Radiosurgery and [8]Unit of Neuroradiology, Humanitas Clinical and Research Center - IRCCS, Rozzano, Milan; [9]Neuroradiology Unit and CERMAC, Vita-Salute San Raffaele University and IRCCS San Raffaele Scientific Institute, Milan; [10]Faculty of Psychology, Università di Milano Bicocca, Milan; [11]Department of Biomedical Sciences, Humanitas University, Rozzano; [12]Unit of Nuclear Medicine, Humanitas Clinical and Research Center -IRCCS, Rozzano, Milan; and [13]Department of Neuro-Oncology, University and City of Health and Science Hospital, Turin, Italy

To whom correspondence should be addressed: Marco Riva, M.D. [E-mail: marco.riva@unimi.it]

Marco Riva and Egesta Lopci contributed equally to the present study.

Citation: World Neurosurg. (2019) 126:e270-e280.
https://doi.org/10.1016/j.wneu.2019.02.031

*Journal homepage: **www.journals.elsevier.com/world-neurosurgery***

*Available online: **www.sciencedirect.com***

Table 1. Clinical and Demographic Characteristics

Characteristic	Value
Sex (*n*)	
Male	61
Female	45
Age (years)	44.01 ± 13.7
Treatment-naive subjects (*n*)	48
Histologic type and grade (*n*)	
Grade II	45
Oligodendroglioma	26
Astrocytoma	8
Oligoastrocytoma	11
Grade III	51
Anaplastic oligodendroglioma	15
Anaplastic astrocytoma	22
Anaplastic oligoastrocytoma	14
MRI lesion volume (cm^3)	
Mean	29.1
Range	1.1–232.1
Lesion side (*n*)	
Right	46
Left	50
MRI enhancement (*n*)	
Present	27
Absent	69

MRI, magnetic resonance imaging.

Conventional MRI has been the standard modality for the preoperative characterization of a primary brain tumor.[4,5] However, LGGs often show the absence of contrast enhancement in the early stages of progression, which can lead to an underestimation of the tumor grade.[4,6] Positron emission tomography (PET) with radiolabeled amino acids, such as L-methyl-C11-methionine (11C-METH), has been proved to be a valuable tool for the characterization of brain tumors in vivo. It has been shown that 11C-METH PET can differentiate gliomas,[7-11] can provide prognostic information before surgery,[8,12-15] can be used for radiation therapy planning,[16,17] and is highly diagnostically accurate in the detection of glioma recurrence.[18] With these findings, several international working groups, such as the Response Assessment in Neuro-Oncology and the European Association of Neuro-Oncology, have recommended the additional use of amino acid PET imaging at every stage of brain tumor management.[19,20]

Nevertheless, few studies have evaluated the correlations between the semiquantitative and qualitative metrics of 11C-METH PET and the clinical, radiological, histological, and molecular features of LGGs. The aim of the present observational study was, thus, to characterize the relationships between 11C-METH PET metrics, conventional MRI parameters, histological and molecular factors, and the clinical features of patients undergoing surgical resection of LGGs.

Table 2. Nonenhancing Lower Grade Gliomas on Magnetic Resonance Imaging and Positron Emission Tomography Semiquantitative Parameters

Grade	SUVmax	SUV Ratio	MTB
II	2.4 ± 1.2	1.7 ± 0.6	7.1 ± 0.9
III	3.6 ± 1.4	2.2 ± 0.6	28.8 ± 1.0
P value	0.001	0.003	<0.001

Data presented as mean ± standard deviation.
SUVmax, maximum standardized uptake value; SUV, standardized uptake value; MTB, metabolic tumor burden.

METHODS

Patient Population

A series of 96 patients (51 men, 45 women; age, 44.1 ± 13.7 years) affected by LGG (i.e., grade II and III), who had undergone craniotomy for tumor resection from March 2012 to January 2015, was analyzed in the present observational cohort study (ClinicalTrials.gov identifier, NCT02518061). All patients underwent 11C-METH PET within 30 days before surgery, had adequate tumor specimen examination after surgery, and had fully available clinical data, including complete follow-up data. The demographic data and clinical and radiological features are reported in **Table 1**. The pathological diagnosis was performed in accordance with the 2007 WHO brain tumor classification.[21] The local ethics committee approved the present study (approval no. 1481).

11C-METH PET Imaging

All patients underwent 11C-METH PET before surgery. The radiopharmaceutical carrier-free L-(methyl-11C)-methionine was synthesized on-site using a General Electric TracerLab FXc synthesis module (General Electric Healthcare, Waukesha, Wisconsin, USA) using a previously described method.[8] A total of 300–500 MBq was administered to patients who had been fasting for ≥4 hours. Images were acquired 15 minutes later using a PET/computed tomography (CT) scanner, either a Biograph 6 LSO scanner (Siemens Medical Systems, Erlangen, Germany) or a Discovery 690 GE scanner (General Electric Healthcare). CT attenuation-corrected 3-dimensional images were acquired for 10 minutes from the scalp to vertebra C3, and the images were subsequently reconstructed using an iterative reconstruction algorithm (ordered subset expectation maximization) and displayed using the Adw4.6 Workstation (GE Healthcare). The images were reconstructed and acquired to minimize differences in the semiquantitative evaluations related to the use of 2 different scanners.

The data obtained by 11C-METH PET were analyzed by board-certified nuclear medicine physicians and then revised using a semiquantitative scale. The maximum standardized uptake value (SUVmax), SUV ratio, and metabolic tumor burden (MTB) were

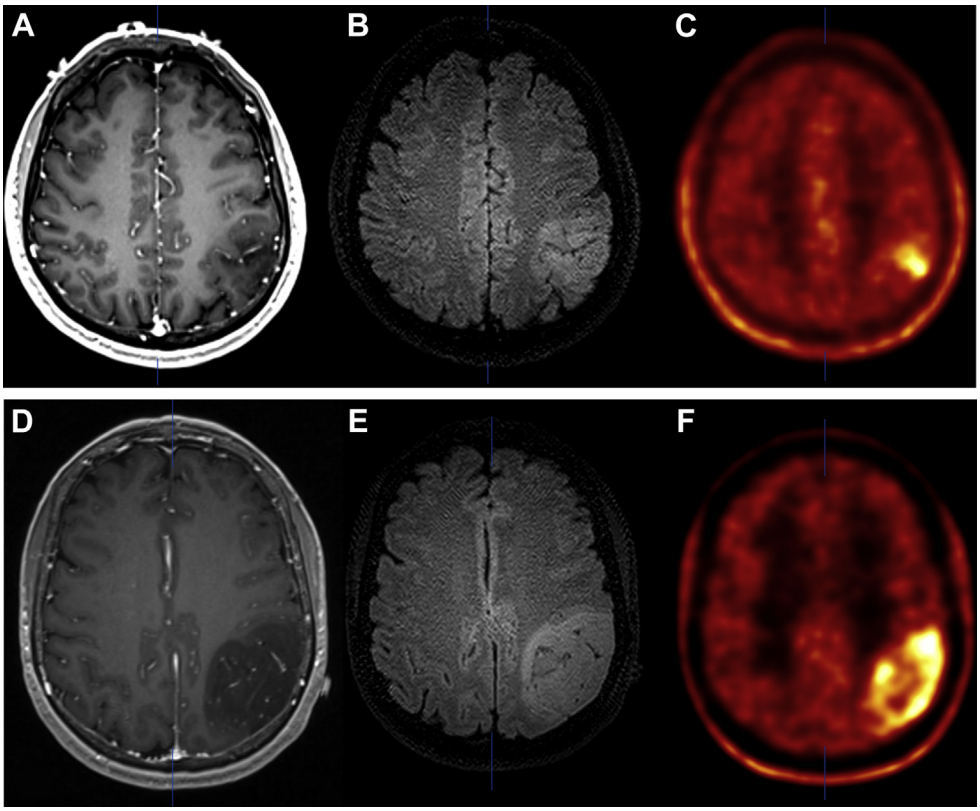

Figure 1. Positron emission tomography (PET) metrics in a nonenhancing lower grade glioma. (**A**) Preoperative T1-weighted image after contrast injection, (**B**) fluid-attenuated inversion recovery image, and (**C**) carbon-11-methionine (11C-METH) PET scan of a patient with a grade II, isocitrate dehydrogenase (IDH)-1 mutated and 1p19q codeleted oligoastrocytoma. Magnetic resonance imaging (MRI) showed no enhancement and a volume of 30.2 cm^3. The maximum standardized uptake value (SUV) was 2.2, the SUV ratio was 1.7, and metabolic tumor burden was 15.1. (**D**–**F**) Although the lesion had an overlapping MRI phenotype, with no contrast enhancement and an MRI volume of 40.1 cm^3, the PET metrics were higher (maximum SUV, 2.7; SUV ratio, 1.8; metabolic tumor burden, 29.2) in a patient with a final diagnosis of a grade III oligoastrocytoma, IDH-1/2 wild-type, with no 1p19q codeletion. PET also depicted a structural heterogeneity according to the metabotype, documenting several hypermetabolic foci within the lesion with a homogenous fluid-attenuated inversion recovery MRI appearance.

considered semiquantitative parameters. The SUV ratio was the ratio between the count rates determined in the region of interest (ROI) drawn in the tumor area with the highest uptake of 11C-METH (SUVmax) and the count rate in a corresponding ROI drawn on the contralateral side. The values were corrected for injected activity and adjusted to patient weight. The tumor volumes found on PET were then delineated automatically using a dedicated workstation software package (PETVCAR [PET volume computer assisted reading]; GE Healthcare), with an estimated threshold weight of 50%. When needed, the volume was manually adjusted using visual thresholding. MTB was computed as the volume (expressed in cm^3) delineated on 11C-METH PET images by the ROI of the entire tumor extent.

MRI Evaluation

Volumetric MRI sequences were acquired preoperatively for all patients with a 3 Tesla MRI scanner (Siemens Verio, Erlangen, Germany) on the day before surgery. Image evaluation was performed by a board-certified neuroradiologist, who was kept unaware of the nuclear medicine data. The volumes were computed using the iPlan Cranial 3.0 software suite (Brainlab AG, Munich, Germany) from T2-weighted hyperintense lesions on fluid-attenuated inversion recovery and gadolinium-enhancing T1-weighted lesions by manual delineation of the lesion borders on all involved slices. The preoperative MRI data set was coregistered with a CT head scan using 7 radiolucent fiducial markers and the 11-C-METH-PET with iPlan Cranial 3.0 software (Brainlab). The coregistered data set was then available for image guidance during surgery using a neuronavigation platform (Brainlab Curve [Brainlab AG]).

Surgical Protocol

All the patients gave written informed consent for the surgical procedure. Surgery was performed with the aid of multimodal

Table 3. Discrimination of Grade With Positron Emission Tomography, Magnetic Resonance Imaging, and Multimodal Metrics and Identification of Cutoff Values in Discriminating Lower Grade Gliomas

Variable	Cutoff	Accuracy (%)	Sensitivity (%)	Specificity (%)
SUVmax	2.7	67.8	55.6	78.4
SUV ratio	2.0	71.9	71.1	72.5
MTB	14.9	67.8	64.4	70.6
Gd enhancement	NA	69.8	95.6	47.1

Magnetic resonance imaging features (e.g., presence of gadolinium enhancement) obtained from this cohort reported for comparison.
SUVmax, maximum standardized uptake value; SUV, standardized uptake value; MTB, metabolic tumor burden; Gd, gadolinium; NA, not applicable.

electrophysiological monitoring and intraoperative stimulation mapping for motor and language functions, with either asleep or awake anesthesia according to the surgical indications.[22,23] An ultrasound machine (Prosound Alpha7 [Hitachi Aloka Medical Ltd., Zurich, Switzerland]) with a precalibrated multifrequency (3.75–10 MHz) convex transducer footprint of 20 mm was used.[24] A rigid array with 3 optic references was mounted onto the transducer to have it integrated with neuronavigation to guide the tissue sampling in vivo and to acknowledge a possible shifting of the ROIs.

Pathological Assessment

Tumor grading was performed on slides after hematoxylin and eosin staining in accordance with the WHO international histological classification of tumors.[21] Isocitrate dehydrogenase (IDH)-1 mutational analysis was conducted with immunohistochemistry using an antibody to IDH R132H, and wild-type cases were then validated by polymerase chain reaction. 1p/19q codeletion status was assessed using fluorescence in situ hybridization (Vysis 1p36/1q25 and 19q13/19p13 [Abbot Molecular, Chicago, Illinois, USA). Deletions of 1p and 19q were defined as 33% of tumor nuclei containing the loss of heterozygosity pattern. The integrated diagnosis of the histopathological grade and molecular profiles are reported in **Supplemental Table 1**. The cell proliferation index was measured using immunohistochemistry and the MIB-1 antibody against Ki-67 protein.

Table 4. Accuracy, Sensitivity, and Specificity of Multimodal Characterization, Combining Positron Emission Tomography Semiquantitative Metrics and Magnetic Resonance Imaging Features (Gadolinium Enhancement)

Variable	Accuracy (%)	Sensitivity (%)	Specificity (%)
SUVmax	70.8	84.4	58.9
SUV ratio	70.8	86.7	56.9
MTB	76.0	86.7	66.7

SUVmax, maximum standardized uptake value; SUV, standardized uptake value; MTB, metabolic tumor burden.

Statistical Analysis

Analysis of variance was used to explore the relationship among the PET metrics, as measured by semiquantitative parameters, and the clinical and radiological features. The differences between rates were compared using χ^2 analysis. The t test was used to investigate the differences between scanners (Siemens vs. GE Healthcare) for the semiquantitative parameters.

To investigate the relationship between metabolic metrics and the 3 molecular subgroups, PET metrics were analyzed using analysis of variance on the natural log of the dependent variable (F test) and with a nonparametric Kruskal-Wallis test because of distributional concerns.

For rank correlation, Spearman's correlation coefficient (rho) and a linear regression test were used. The sensitivity, specificity, and accuracy in characterizing the tumor grade (i.e., grade II vs. III) were computed to estimate the power of each parameter to discriminate between the 2 grades. A study of the optimal cutoff and the accuracy was then performed using receiver operating characteristic curve analysis. Multivariate analysis was performed to test the relationship among the PET semiquantitative parameters and other radiological and molecular features. Statistical significance was set at $P \leq 0.05$ for each evaluation.

RESULTS

PET Semiquantitative Metrics and Histological Grade

Using the 2007 WHO classification, the distribution of brain tumors was as follows: 26 grade II and 15 grade III oligodendrogliomas, 8 grade II and 22 grade III astrocytomas, and 11 grade II and 14 grade III oligoastrocytomas. Of the 96 patients, 48 were treatment naive, with newly diagnosed lesions, and 48 had recurrent tumors (**Table 1**).

The mean proliferative index, as measured by MIB-1, was different among the 2 grades (i.e., 3.0 for grade II and 13.3 for grade III; $P < 0.001$). The proliferative index was related to the SUVmax [$F(1,92) = 4.3$; $P = 0.04$], SUV ratio [$F(1,92) = 4.2$; $P = 0.04$], and MTB [$F(1,92) = 9.8$; $P = 0.002$].

The mean SUVmax was 3.5 ± 1.7 (range, 1.0–9.2), the mean SUV ratio was 2.3 ± 1.1 (range, 1.1–8.3), and the mean MTB was 33.13 (range, 0.3–250.3). No difference was found between the 2 scanners for all semiquantitative parameters ($P > 0.05$). When analyzed with respect to the tumor grade, a statistically significant difference was observed for SUVmax, SUV ratio, and MTB between grades II and III. In particular, the tumor grade correlated with SUVmax [$F(1,94) = 18.56$; $P < 0.001$], SUV ratio [$F(1,94) = 13.46$; $P < 0.01$], and MTB [$F(1,94) = 21.58$; $P < 0.0001$), with grade III lesions having higher values for all metrics (**Supplemental Figure 1**).

PET Semiquantitative Metrics and MRI Findings

On the preoperative MRI studies, 69 patients had no enhancement and 27 had a variable degree of enhancement (**Table 1**). Patients with contrast enhancement had significantly greater PET semiquantitative values statistically. The SUVmax

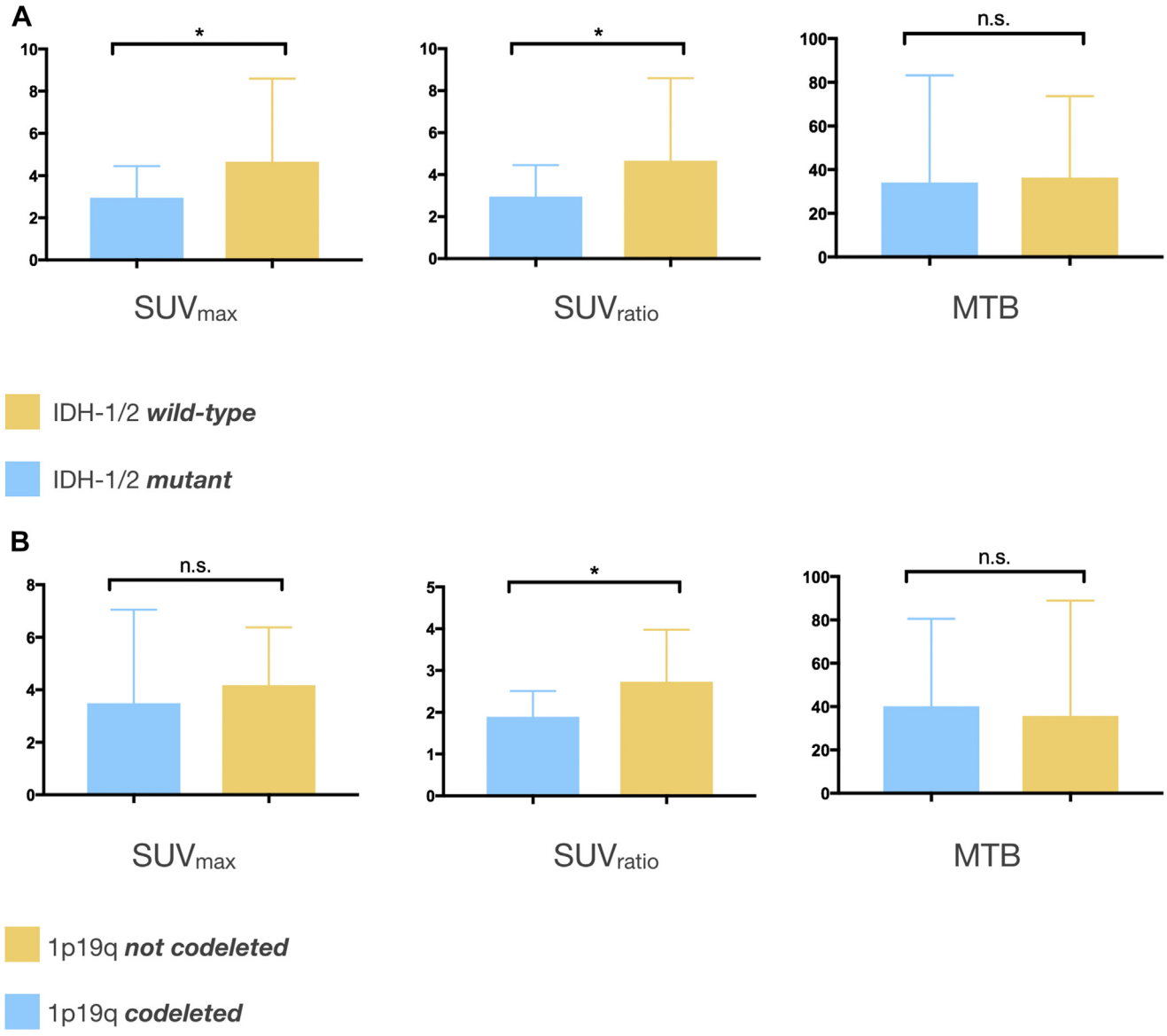

Figure 2. Relationship between positron emission tomography (PET) metrics and molecular markers. (**A**) The maximum standardized uptake value (SUV) and SUV ratio but not the metabolic tumor burden were significant greater statistically in the isocitrate dehydrogenase wild-type lesion compared with the mutated counterparts. (**B**) In contrast, the SUV ratio was lower in lower grade gliomas with 1p19q codeletion. *$P < 0.01$. n.s., not statistically significant.

[F(1.94) = 15.4; P < 0.001], SUV ratio [F(1.94) = 12.4; P = 0.001], and MTB [F(1.94) = 6.9; P = 0.01) were all related to gadolinium enhancement.

Among the nonenhancing LGGs (69 patients; Table 2), SUVmax (P = 0.001), SUV ratio (P = 0.003), and MTB (P < 0.001) were all significantly different statistically between the grade II and grade III lesions. The average SUVmax, SUV ratio, and MTB in the nonenhancing grade II LGGs was 2.4 ± 1.2, 1.7 ± 0.6, and 7.1 ± 0.9, respectively. In contrast, the average SUVmax, SUV ratio, and MTB was 3.6 ± 1.4, 2.2 ± 0.6, and 28.8 ± 1.0 for nonenhancing grade III LGGs. Representative examples are shown in Figure 1.

The MRI lesion volume correlated only with the MTB value [F(1.93) = 9.9; P = 0.002] but not with the SUVmax or SUV ratio. However, the correlation between the MRI volume and MTB was modest (r^2 = 0.13; Supplemental Figure 2).

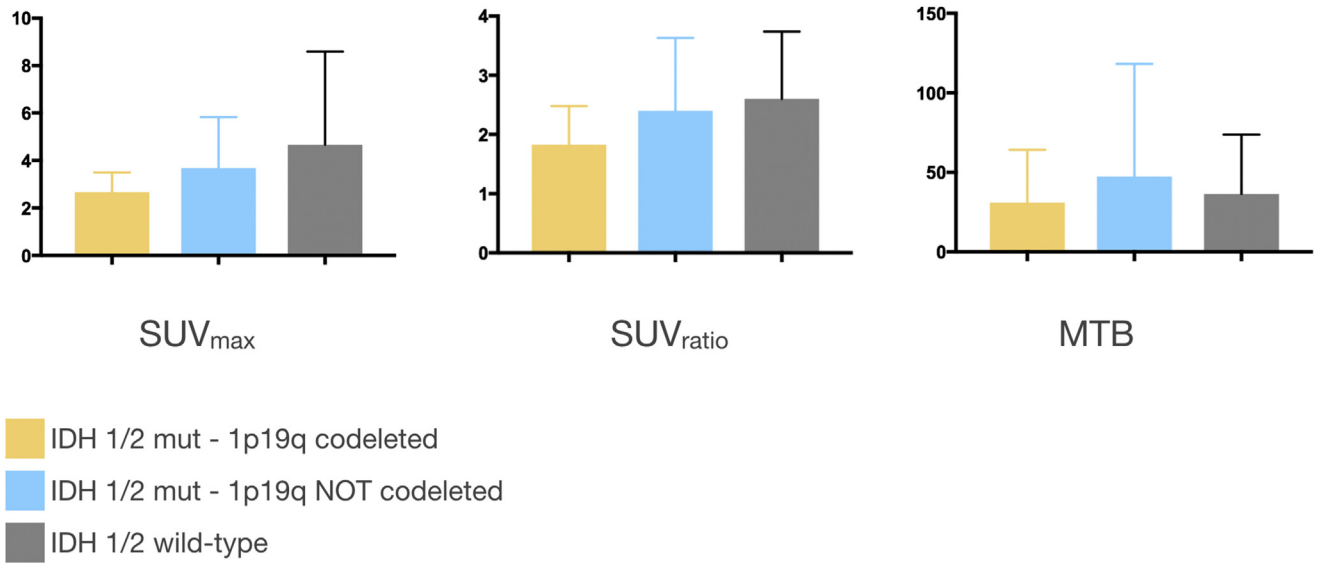

Figure 3. Positron emission tomography metrics and molecular integrated diagnosis of lower grade gliomas. Despite a trend with the maximum standardized uptake value and standardized uptake value ratio, none of the positron emission tomography metrics measured reached a statistically significant threshold when the lower grade gliomas of the present cohort were partitioned according to the molecular features, as recommended by the recently updated World Health Organization brain tumor classification.

Accuracy, Sensitivity, and Specificity of Lesion Characterization by PET and MRI

The accuracy, sensitivity, and specificity of the 3 PET measurements in discriminating between grades II and III were evaluated. The results showed good accuracy overall, especially for the specificity. The tumor grade was significantly predicted by the SUVmax ($P < 0.001$), SUV ratio ($P = 0.002$), and MTB ($P < 0.001$). The optimal cutoff value was 2.7, 2.0, and 14.9 for the SUVmax, SUV ratio, and MTB, respectively (Table 3).

An additional analysis was performed to assess whether the combination of the PET parameters and MRI features (i.e., the presence of contrast enhancement) would improve the diagnostic accuracy for discriminating between grades II and III. We found that the likelihood of a grade III lesion was greater when contrast enhancement and greater PET semiquantitative values were both present. An overall gain in accuracy, sensitivity, and specificity was observed (Table 4) compared with the MRI or PET findings alone.

PET Semiquantitative Metrics and Molecular Features

The relationships between the metabolic parameters and molecular features were explored, constraining the analysis to the newly diagnosed lesions. Both the SUVmax and the SUV ratio were significantly greater ($P < 0.05$) in IDH-1/2 wild-type lesions ($n = 28$) compared with mutated lesions ($n = 20$; Figure 2A). In addition, the SUV ratio was associated with the presence of a 1p19q codeletion only, with lesions with 1p19q codeletion having a lower SUV ratio (Figure 2B).

On multivariate analysis, only the SUVmax was found to correlate significantly with the IDH status ($P = 0.02$). The other parameters (e.g., SUV ratio, histological grade, and contrast enhancement), were not associated with the mutational status of IDH.

A positive trend toward a correlation between the PET semiquantitative metrics and the 3 molecular subgroups of the new 2016 WHO classification (i.e., IDH-1/2 mutated and 1p19 codeletion, IDH-1/2 mutated and no 1p19q codeletion, and IDH-1/2 wild-type lesions) was evident, but the difference was not statistically significant (Figure 3).

DISCUSSION

LGGs display a variable prognosis that can be predicted by the molecular factors,[3,20] in addition to the clinical variables, such as patient age at diagnosis,[25] tumor volume,[26] growth rate,[27] and surgical resection extent.[26,28] The updated WHO classification of the central nervous system tumors of 2016 now includes both conventional histological parameters and molecular factors in an integrated diagnosis.[1] In particular, IDH status and 1p/19q codeletion have been shown to capture the biologic characteristics of LGGs with greater sensitivity compared with histological classification alone,[29] which can be hampered by both interobserver variability and sampling errors during surgery.

PET with radiolabeled amino acids, such as 11C-METH, has been proved to be a valuable tool for the in vivo characterization of primary brain tumors.[30] 11C-METH PET can discriminate high- and low-grade gliomas,[7-11] provide prognostic information before surgery,[12-15,31] and be used for radiation therapy planning.[16,17] It also has high diagnostic accuracy in the detection of glioma recurrence.[18]

Based on a previous investigation,[8] the present study evaluated the additional benefit of metabolic imaging with 11C-METH-PET in the management of LGGs. Gliomas are heterogeneous tumors.[32-34] Thus, the identification of the extent of infiltration

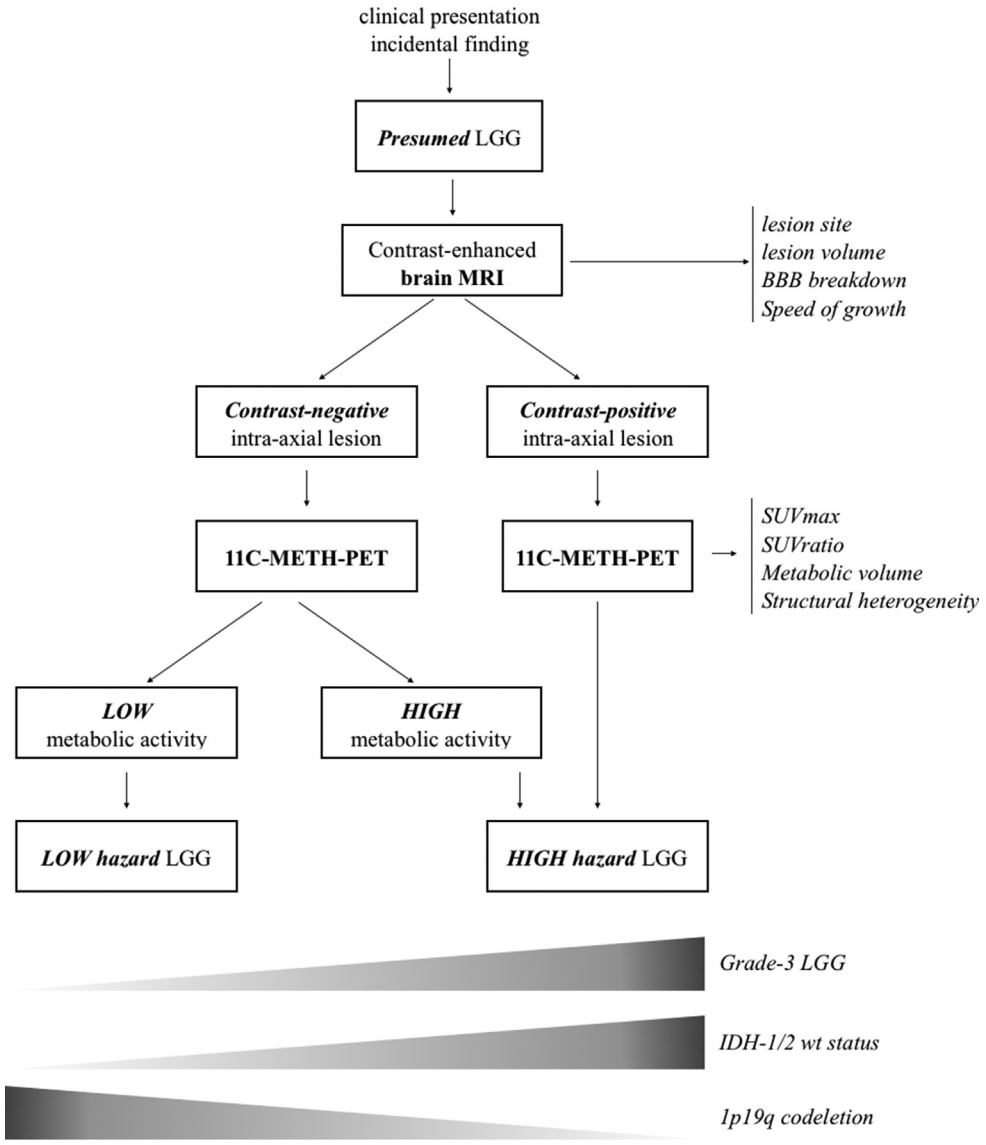

Figure 4. Multimodal preoperative characterization of lower grade gliomas. The results of the present study could be used to discuss the role of amino acid positron emission tomography in the preoperative evaluation of lower grade gliomas. After presentation, the diagnostic radiological workup should include contrast-enhanced magnetic resonance imaging, which provides relevant morphological data, such as lesion site, volume, signs of blood–brain barrier breakdown (shown as contrast enhancement) and growth rate, when serial scans are volumetrically analyzed. Amino acid positron emission tomography could integrate these data with semiquantitative metrics and a qualitative depiction of the structural heterogeneity. Using the metabolic activity measured from the lesion, this multimodal radiological evaluation could help identify low- and high-risk lesions, with the latter being those more likely to have more aggressive behavior as shown by their histopathology (i.e., grade III) and molecular status (isocitrate dehydrogenase wild-type). Finally, this information could support clinical decision making, including the timing of therapeutic intervention and guidance of proper tissue sampling to minimize lesion understaging. High-risk lesions should receive prompt treatment, and low-risk lesions could undergo close follow-up magnetic resonance imaging scans to assess the growth rate for a more refined tailoring of the treatment options.

and of aggressive tumor components is relevant in planning the surgery and sampling the most representative tissue for a correct diagnosis. In this regard, conventional MRI has limited usefulness in the definition of the heterogeneity and extension of gliomas. Therefore, it has been questioned whether structural imaging alone will be able to appropriately guide the resection and the sampling appropriately or whether metabolic imaging should also be included, especially for nonenhancing lesions.[35] The Response

Assessment in Neuro-Oncology Working Group[19] and the European Association of Neuro-Oncology[20] have both recommended the use of amino acid PET as an additional tool for evaluating gliomas.

To date, few studies have investigated the correlations of metabolic and structural MRI findings with the molecular features and histological grade in LGGs.[36,37] Among these studies, only a few have examined the imaging findings in the context of the new WHO brain tumor classification.[8,14,38]

The pathological diagnosis was determined using the 2007 WHO classification.[21] However, given the retrospective design, which represents a limitation of the present observational study, a robust relationship between the glioma grade and 11C-METH PET semiquantitative metrics was found in several aspects. Thus, imaging with 11C-METH PET can help in the distinction of nonenhancing gliomas on MRI between grade II and grade III. Also, greater SUVmax, SUV ratio, and MTB values were significantly associated with grade III lesions compared with grade II lesions.

No significant correlation was found between the MRI volume and PET metrics (**Supplemental Figure 2**). This was not surprising because the anaplastic areas that can be detected by PET coexist with more differentiated areas without modifying the MRI volume of the LGGs. The metabolic findings could, thus, be regarded as an additional noninvasive in vivo preoperative biomarker of LGGs aggressiveness, along with an increase in the lesion volume[26] and the speed of growth.[27]

The combination of 11C-METH PET and conventional MRI enabled a more refined preoperative diagnosis. The diagnostic accuracy, sensitivity, and, to a lower extent, specificity were improved when the findings from 11C-METH PET and conventional MRI were combined, with an accuracy and a specificity as great as 75% and 87%, respectively. The combination of the diagnostic yield of MRI with that of PET, in particular the SUVmax, could be regarded as a promising approach for a better pretreatment evaluation of presumed LGGs (**Figure 4**), especially if combined with the increasing use of hybrid MRI-PET facilities worldwide.[39]

In the present study, we also found a significant association between IDH status and PET parameters, because the IDH-1/2 wild-type lesions displayed greater metabolic activity than IDH-1/2 mutated LGGs in terms of the SUVmax and SUV ratio. In contrast, the lesions with 1p19q codeletion lesions had a lower SUV ratio. The latter finding (i.e., the relationship between the 1p19q loss of heterozygosity and PET metrics) can appear controversial when compared with earlier studies,[14] in which LGGs with 1p19q codeletion displayed higher uptake of PET tracers. However, a more recent study found that 11C-METH PET metrics were significantly greater in oligodendroglial lesions without 1p/19q deletion, especially when the tumor/normal brain ratio was analyzed,[38] as in the present study. This discrepancy could be explained by several factors, including the heterogeneity of different clinical cohorts and the different percentages of true astrocytic and oligodendroglial lesions.[40] In addition, it could be argued that tumors without 1p/19q deletion are less likely to have an IDH-1 mutation, which could lead to more active metabolism than that in those with deletions.[2,40]

When we analyzed the 3 molecular subgroups, we restricted the analysis to newly diagnosed lesions. IDH-1/2 wild-type lesions displayed greater metabolic activity compared with IDH-mutated lesions with 1p19 codeletion and IDH-mutated lesions without 1p19q codeletion, as measured using the SUVmax and SUV ratio. However, the difference did not reach statistical significance. This could have been because of the small number of patients in each subgroup or the high relative fraction of IDH wild-type lesions. Further studies are, thus, needed to prove whether these interesting preliminary findings can be confirmed with a greater sample size and, hopefully, with a prospective design,[41] using the new WHO brain tumor classification.

Some attention must be given to the acquisition protocols and reconstruction algorithms, in particular, in the context of multiple scanner types or multicenter settings, because the inter- and intracenter comparability of PET data should be based on harmonized criteria. In addition, when a robust correlation between the imaging data and patient pathological features has been demonstrated, quantitative diagnostic findings could guide the choice of the site of tissue sampling, such as occurred in the present study, in which samples from hypermetabolic areas were sent for histopathological diagnosis separately. This approach could reduce the errors in the histopathological evaluation that result from both sampling errors and interobserver variability.[42]

CONCLUSION

The results from the present observational study have provided further evidence of the diagnostic power of 11C-MET PET in providing a refined preoperative evaluation of patients affected by presumed LGGs, although retrospectively. The information we found on the metabolism of the lesions has potential clinical impact for guiding treatment decisions[43] in a patient-specific approach,[44] adding relevant clues about the site of tissue sampling for a proper integrated histomolecular diagnosis.

PET imaging and the derived semiquantitative metrics should, thus, be considered relevant, on a par with the findings from other imaging techniques such as advanced MRI, to improve the noninvasive in vivo characterization of LGGs and, ultimately, to promote improved care and outcomes for patients.

REFERENCES

1. Louis DN, Perry A, Reifenberger G, et al. The 2016 World Health Organization classification of tumors of the central nervous system: a summary. *Acta Neuropathol*. 2016;1311:803-820.
2. Brat DJ, Verhaak RG, Aldape KD, et al. Comprehensive, integrative genomic analysis of diffuse lower-grade gliomas. *N Engl J Med*. 2015;372:2481-2498.
3. Aoki K, Nakamura H, Suzuki H, et al. Prognostic relevance of genetic alterations in diffuse lower-grade gliomas. *Neuro Oncol*. 2018;20:66-77.
4. Law M, Yang S, Wang H, et al. Glioma grading: sensitivity, specificity, and predictive values of perfusion MR imaging and proton MR spectroscopic imaging compared with conventional MR imaging. *AJNR Am J Neuroradiol*. 2003;24:1989-1998.
5. Castellano A, Falini A. Progress in neuro-imaging of brain tumors. *Curr Opin Oncol*. 2016;28:484-493.
6. Plotkin M, Blechschmidt C, Auf G, et al. Comparison of F-18 FET-PET with F-18 FDG-PET for biopsy planning of non-contrast-enhancing gliomas. *Eur Radiol*. 2010;20:2496-2502.

7. Herholz K, Hölzer T, Bauer B, et al. 11C-methionine PET for differential diagnosis of low-grade gliomas. *Neurology*. 1998;50:1316-1322.

8. Lopci E, Riva M, Olivari L, et al. Prognostic value of molecular and imaging biomarkers in patients with supratentorial glioma. *Eur J Nucl Med Mol Imaging*. 2017;44:1155-1164.

9. Shinozaki N, Uchino Y, Yoshikawa K, et al. Discrimination between low-grade oligodendrogliomas and diffuse astrocytoma with the aid of 11C-methionine positron emission tomography. *J Neurosurg*. 2011;114:1640-1647.

10. Singhal T, Narayanan TK, Jacobs MP, Bal C, Mantil JC. 11C-methionine PET for grading and prognostication in gliomas: a comparison study with 18F-FDG PET and contrast enhancement on MRI. *J Nucl Med*. 2012;53:1709-1715.

11. Kato T, Shinoda J, Oka N, et al. Analysis of ^{11}C-methionine uptake in low-grade gliomas and correlation with proliferative activity. *AJNR Am J Neuroradiol*. 2008;29:1867-1871.

12. Galldiks N, Stoffels G, Ruge MI, et al. Role of O-(2-18F-fluoroethyl)-L-tyrosine PET as a diagnostic tool for detection of malignant progression in patients with low-grade glioma. *J Nucl Med*. 2013;54:2046-2054.

13. Pauleit D, Floeth F, Hamacher K, et al. O-(2-[18F] fluoroethyl)-L-tyrosine PET combined with MRI improves the diagnostic assessment of cerebral gliomas. *Brain*. 2005;128:678-687.

14. Saito T, Maruyama T, Muragaki Y, et al. ^{11}C-methionine uptake correlates with combined 1p and 19q loss of heterozygosity in oligodendroglial tumors. *AJNR Am J Neuroradiol*. 2013;34:85-91.

15. Kim S, Chung J-K, Im S-H, et al. 11C-methionine PET as a prognostic marker in patients with glioma: comparison with 18F-FDG PET. *Eur J Nucl Med Mol Imaging*. 2005;32:52-59.

16. Langen K-J, Galldiks N, Hattingen E, Shah NJ. Advances in neuro-oncology imaging. *Nat Rev Neurol*. 2017;13:279-289.

17. Navarria P, Reggiori G, Pessina F, et al. Investigation on the role of integrated PET/MRI for target volume definition and radiotherapy planning in patients with high grade glioma. *Radiother Oncol*. 2014;112:425-429.

18. Nariai T, Tanaka Y, Wakimoto H, et al. Usefulness of l-[methyl-11C] methionine—positron emission tomography as a biological monitoring tool in the treatment of glioma. *J Neurosurg*. 2005;103:498-507.

19. Albert NL, Weller M, Suchorska B, et al. Response assessment in neuro-oncology working group and European association for neuro-oncology recommendations for the clinical use of PET imaging in gliomas. *Neuro Oncol*. 2016;18:1199-1208.

20. Weller M, van den Bent M, Tonn JC, et al. European Association for Neuro-Oncology (EANO) guideline on the diagnosis and treatment of adult astrocytic and oligodendroglial gliomas. *Lancet Oncol*. 2017;18:e315-e329.

21. Louis DN, Ohgaki H, Wiestler OD, et al. The 2007 WHO classification of tumours of the central nervous system. *Acta Neuropathol*. 2007;114:97-109.

22. Bello L, Riva M, Fava E, et al. Tailoring neurophysiological strategies with clinical context enhances resection and safety and expands indications in gliomas involving motor pathways. *Neuro Oncol*. 2014;16:1110-1128.

23. Riva M, Fava E, Gallucci M, et al. Monopolar high-frequency language mapping: can it help in the surgical management of gliomas? A comparative clinical study. *J Neurosurg*. 2016;124:1479-1489.

24. Riva M, Hennersperger C, Milletari F, et al. 3D intra-operative ultrasound and MR image guidance: pursuing an ultrasound-based management of brainshift to enhance neuronavigation. *Int J Comput Assist Radiol Surg*. 2017;12:1711-1725.

25. Chang EF, Smith JS, Chang SM, et al. Preoperative prognostic classification system for hemispheric low-grade gliomas in adults. *J Neurosurg*. 2008;109:817-824.

26. Smith JS, Chang EF, Lamborn KR, et al. Role of extent of resection in the long-term outcome of low-grade hemispheric gliomas. *J Clin Oncol*. 2008;26:1338-1345.

27. Pallud J, Blonski M, Mandonnet E, et al. Velocity of tumor spontaneous expansion predicts long-term outcomes for diffuse low-grade gliomas. *Neuro Oncol*. 2013;15:595-606.

28. Riva M, Bello L. Low-grade glioma management: a contemporary surgical approach. *Curr Opin Oncol*. 2014;26:615-621.

29. Eckel-Passow JE, Lachance DH, Molinaro AM, et al. Glioma groups based on 1p/19q, *IDH*, and *TERT* promoter mutations in tumors. *N Engl J Med*. 2015;372:2499-2508.

30. Herholz K, Coope D, Jackson A. Metabolic and molecular imaging in neuro-oncology. *Lancet Neurol*. 2007;6:711-724.

31. Galldiks N, Kracht LW, Berthold F, et al. [11C]-L-methionine positron emission tomography in the management of children and young adults with brain tumors. *J Neurooncol*. 2010;96:231-239.

32. Johnson BE, Mazor T, Hong C, et al. Mutational analysis reveals the origin and therapy-driven evolution of recurrent glioma. *Science*. 2014;343:189-193.

33. Inano R, Oishi N, Kunieda T, et al. Visualization of heterogeneity and regional grading of gliomas by multiple features using magnetic resonance-based clustered images. *Sci Rep*. 2016;6:30344.

34. Castellano A, Donativi M, Rudà R, et al. Evaluation of low-grade glioma structural changes after chemotherapy using DTI-based histogram analysis and functional diffusion maps. *Eur Radiol*. 2016;26:1263-1273.

35. Keunen O, Taxt T, Grüner R, et al. Multimodal imaging of gliomas in the context of evolving cellular and molecular therapies. *Adv Drug Deliv Rev*. 2014;76:98-115.

36. Bette S, Gempt J, Delbridge C, et al. Prognostic value of O-(2-[18F]-Fluoroethyl)-L-tyrosine-positron emission tomography imaging for histopathologic characteristics and progression-free survival in patients with low-grade glioma. *World Neurosurg*. 2016;89:230-239.

37. Verger A, Stoffels G, Bauer EK, et al. Static and dynamic 18F—FET PET for the characterization of gliomas defined by IDH and 1p/19q status. *Eur J Nucl Med Mol Imaging*. 2018;45:443-451.

38. Iwadate Y, Shinozaki N, Matsutani T, Uchino Y, Saeki N. Molecular imaging of 1p/19q deletion in oligodendroglial tumours with 11C-methionine positron emission tomography. *J Neurol Neurosurg Psychiatry*. 2016;87:1016-1021.

39. Bailey DL, Pichler BJ, Gückel B, et al. Combined PET/MRI: from status quo to status go. Summary report of the Fifth International Workshop on PET/MR imaging; February 15-19, 2016; Tübingen, Germany. *Mol Imaging Biol*. 2016;18:637-650.

40. Lopci E. The simplest explanation is usually the correct one—can Occam's razor be applied for diffuse astrocytoma and paradoxical amino acid metabolism? *Eur J Nucl Med Mol Imaging*. 2017;44:1411-1412.

41. Suchorska B, Giese A, Biczok A, et al. Identification of time-to-peak on dynamic 18F-FET-PET as a prognostic marker specifically in IDH1/2 mutant diffuse astrocytoma. *Neuro Oncol*. 2018;20:279-288.

42. Gillies RJ, Kinahan PE, Hricak H. Radiomics: images are more than pictures, they are data. *Radiology*. 2016;278:563-577.

43. van den Bent MJ, Baumert B, Erridge SC, et al. Interim results from the CATNON trial (EORTC study 26053-22054) of treatment with concurrent and adjuvant temozolomide for 1p/19q non-codeleted anaplastic glioma: a phase 3, randomised, open-label intergroup study. *Lancet*. 2017;390:1645-1653.

44. Collins FS, Varmus H. A new initiative on precision medicine. *N Engl J Med*. 2015;372:793-795.

Conflict of interest statement: M. Riva was supported by the Fellowship for Abroad 2013 of the Fondazione Italiana per la Ricerca sul Cancro. The remaining authors declare that the article content was composed in the absence of any commercial or financial relationships that could be construed as a potential conflict of interest.

Received 14 October 2018; accepted 2 February 2019

Citation: World Neurosurg. (2019) 126:e270-e280.
https://doi.org/10.1016/j.wneu.2019.02.031

Journal homepage: ***www.journals.elsevier.com/world-neurosurgery***

Available online: ***www.sciencedirect.com***

1878-8750/$ - see front matter

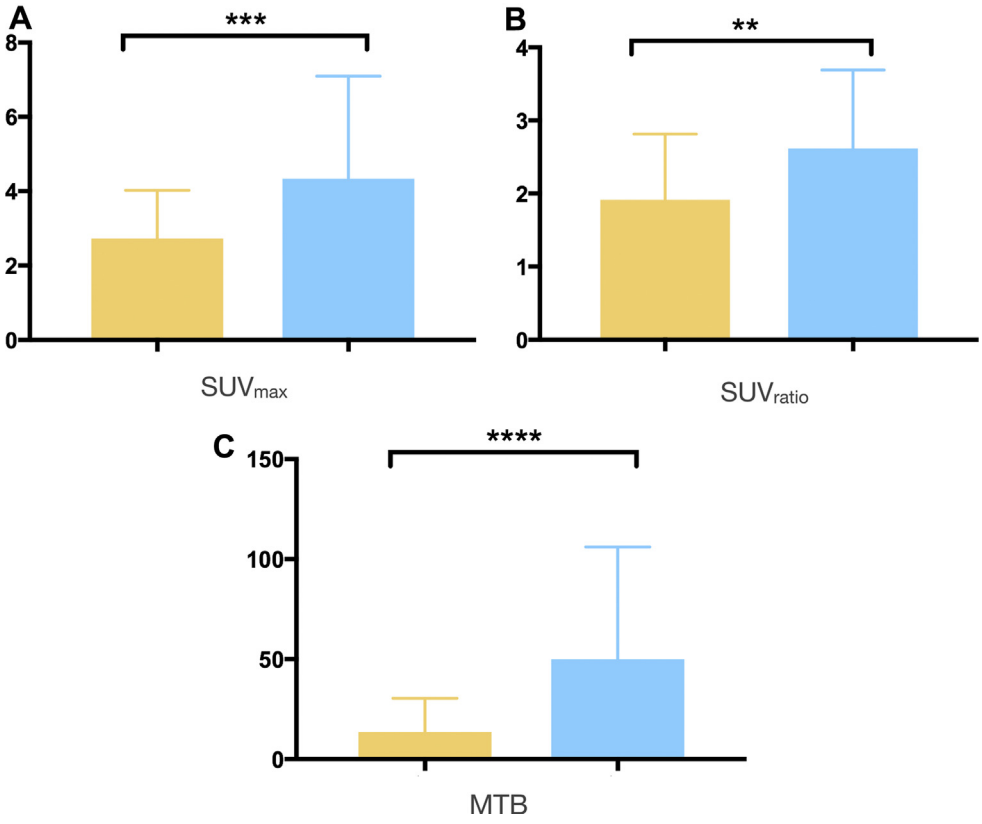

Supplemental Figure 1. Histopathological grade and positron emission tomography semiquantitative metrics. The (**A**) maximum standardized uptake value (SUVmax), (**B**) standardized uptake value (SUV) ratio, and (**C**) metabolic tumor burden (MTB) values were significantly different between grades II and III. $^{**}P < 0.01$; $^{***}P < 0.001$; $^{****}P < 0.0001$. *Yellow* and *blue bars* identify grade II and III lesions, respectively.

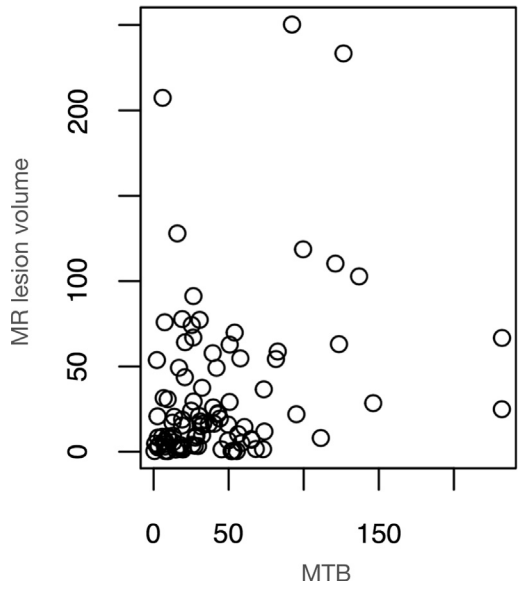

Supplemental Figure 2. Magnetic resonance (MR) imaging lesion volume (cm^3) and metabolic tumor burden (MTB).

Supplemental Table 1. Histopathological Grade and Molecular Profiles: Integrated Diagnosis

Variable	IDH Mutation		
	1p19 Codeletion	No 1p19 Codeletion	Wild Type
Oligodendroglioma ($n = 42$)			
Grade II ($n = 27$)	19 (70.4)	3 (11.1)	5 (18.5)
Grade III ($n = 15$)	9 (60.0)	4 (26.6)	2 (13.4)
Astrocytoma ($n = 29$)			
Grade II ($n = 6$)	1 (16.7)	2 (33.3)	3 (50.0)
Grade III ($n = 23$)	3 (13.0)	8 (34.8)	12 (52.2)
Oligoastrocytoma ($n = 25$)			
Grade II ($n = 11$)	5 (45.4)	3 (27.3)	3 (27.3)
Grade III ($n = 14$)	6 (42.9)	3 (21.4)	5 (35.7)

Data presented as *n* (%).
IDH, isocitrate dehydrogenase.